The Faculty of Arts

Annals of the Faculty of Arts Volume 52 (April-June 2024)
http://www.aafu.journals.ekb.eg
(A Refereed Scientific periodica)

Ain shams university

Digital Geomorphological Mapping of Sabkhas in the Western Gulf of Suez, Egypt

Mohamed El-Raei Mohamed*

The Faculty of Arts- Ain Shams University
mohamed.elraei@art.asu.edu.eg

Abstract:

Digital geomorphological mapping plays a significant role in delineating the boundaries of various phenomena. Some landforms lack distinct transitional boundaries separating them from their surroundings, and these boundaries can change with various climatic conditions. Therefore, automated methods, such as classification and Indicators, are employed to define these boundaries. Sabkhas are a prime example of such landforms, as their boundaries are difficult to determine in the field. Therefore, it is preferable to delineate their boundaries using satellite imagery.

When hearing the term "Sabkha," the mind associates it with soil exhibiting high salinity. In the case of coastal areas, these Sabkhas are typically saturated with water for most of the time. Therefore, it is necessary to apply Indicators of salinity and water or a combination of both to map this phenomenon. It is worth noting that water Indicators, rather than moisture Indicators, were utilized since most Sabkhas have water bodies present for most of the year, unlike vegetation cover, which may not be available throughout the year. The study has developed a new Indicator suitable for accurately mapping Sabkhas.

The study applied these Indicators to a group of Sabkhas located on the western coast of the Gulf of Suez in Egypt

Received: 19/03/2024
Accepted: 25/04/2024
Available online: 30/06/2024

1. Introduction:

A Sabkha is defined as an area of land abundant in marshes, pools, and saline surfaces, enclosed between the shoreline and the interior at varying distances depending on the surface topography and geological formation (Goudie, 2004). Sabkhas form due to the seepage of seawater or groundwater into low-lying areas or areas with high permeability soils. The water often evaporates, leaving behind salt crusts, which are sometimes utilized in salt production.

Several studies aimed to develop automatic methods for extracting Sabkhas from satellite images, but all of them relied on using water and salinity Indicators separately (Douaoui, 2006; Abbas, 2007; Rubab, 2016). Therefore, this study aimed to innovate a new method for extracting Sabkhas from satellite images by integrating water and salinity Indicators into a single Indicator called the SabkhaIndicator. After extracting the Sabkhas from the satellite images, the study focused on morphometric analysis to identify their main characteristics and the factors influencing their formation and development.

The indicators and research methods were applied to the Sabkhas located on the western coast of the Gulf of Suez. The study area's surface is characterized by a gradual decrease from west to east and from south to north. In the south, there are the elevated areas of Al-Malahah and Jebel Zeit. In the west, there are the eastern promontories of the marine and tribal sabkhas, in addition to the eastern promontories of the Ataqa highlands, which have influenced the area's levels and its dentition (Figure 1).

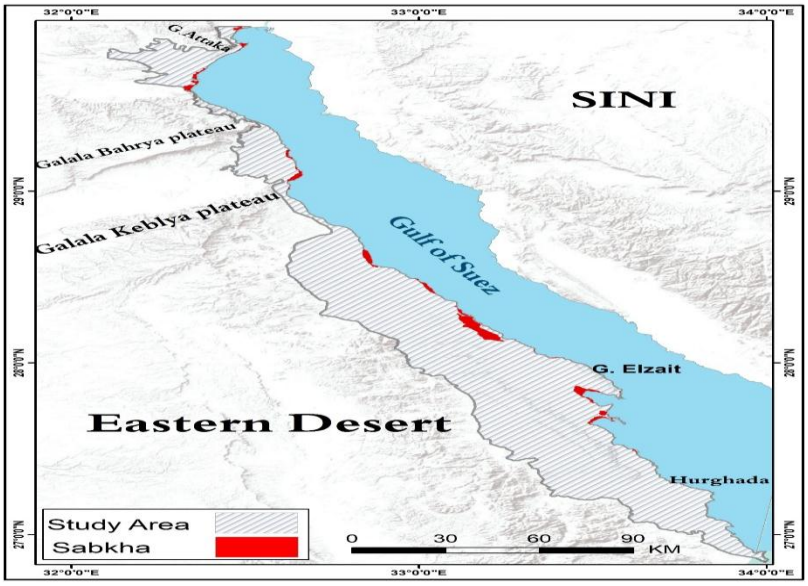

Figure 1: Study area

The coastal plain, in general, is characterized by flatness and lack of dentition, where contour lines are spaced apart in most parts, especially in the areas of lagoons, coastal headlands, and lower sections of the deltas, which are associated with the formation of coastal sabkhas in the region. The lowest point in the study area is found in the Navigation Sabkha at an elevation of -3 m.

Gentle and simple slopes dominate the region, with a slope gradient not exceeding 5 degrees, covering about 85% of the area. Of course, some phenomena only appear in the areas dominated by these slopes, such as deltas and greenish fans. The dominance of these slopes in the coastal area, especially in the lagoon areas, has also had an impact on the formation of marine tongues and sand barriers. This has resulted in the formation of coastal lakes in the region, which quickly dry up and often turn into sabkhas.

2. Data and Research Method:

2.1.Data:

In summary, the study relied on applying a set of Indicators on satellite images, and then comparing the results with topographic maps and interpreting them considering digital elevation models. Therefore, the study relied on satellite images from the European Space Agency's Sentinel-2 satellite, which has a spatial resolution of about 10 meters per Pixel in some bands. It also used a set of 1:50,000 topographic maps produced by the Egyptian Military Survey Authority, and finally, a geological map of the area.

2.2.Methodology:

Phenomena can be identified and extracted from satellite imagery using various methods, including supervised and unsupervised classification, and the use of single-band thresholding and indices. However, using indices is preferred for several reasons, such as ease of application on satellite images from various sources, as well as saving time, and effort, and increasing accuracy.

The idea of an Indicator can be summarized as follows: phenomena are more visible on satellite imagery when captured at specific wavelengths according to the nature of the phenomenon. Therefore, indices maximize the values carried by the image cells captured at the wavelength in which the phenomenon under study appears more clearly than the surrounding phenomena. The application of indices went through several steps, including:

2.2.1. Conversion of Digital Numbers (DN) to Radiance Values in each cell:

Before applying the indices to different satellite images, it is necessary to convert the Digital Number values present in each cell of the imagery to radiance values, using the following equation (Xavier, 2015):

Lλ= ML*Qcal + AL

Lλ= Top of Atmospheric spectral radiance

ML= Band-specific multiplicative rescaling factor from the metadata (Radial multi-band _x, where x is the band number)

AL= Band-specific additive rescaling factor from the metadata (Radiance add bands _x, where x is the band number)

Qcal = Quantized and calibrated standard product pixel values (DN)

After the conversion process, the study tested a set of water and salinity indices to determine the most suitable and effective ones for application in the study area, and to integrate them into a single Indicator for extracting sabkhas from satellite images.

2.2.2. Indicator of salinity

Based on studies that focus on extracting salinity rates and ratios from satellite images, several Indicators have been used, as shown in Table.(1)

Table (1): Salinity Indicators.

Indicator Name	Indicator Equation	Indicator Source
Salt Indicator 1	$\sqrt{R^2 + NIR^2}$	(Khan,2005)
Salt Indicator 2	$\sqrt{R \times B}$	(Khan,2005)
Salt Indicator 3	$\sqrt{R \times G}$	(Khan,2005)
Salt Indicator 4	$\sqrt{G^2 + R^2 + NIR^2}$	(Douaoui,2006)
Salt Indicator 5	$\sqrt{G^2 + R^2}$	(Douaoui, 2006)
Salt Indicator 6	B/R	(Abbas,2007)
Salt Indicator 7	$(B - R)/(B + R)$	(Abbas,2007)
Salt Indicator 8	$(G \times R)/B$	(Abbas,2007)
Salt Indicator 9	$(B \times R)/G$	(Abbas,2007)
Salt Indicator 10	$(R \times NIR)/G$	(Abbas,2007)

Salt Indicator 11	$(G - R + B)/R$	Rubab,2016)(
Salt Indicator 12	$R\ /G$	Rubab,2016)(

NIRNear Infra-red.	R Red.
GGreen.	B Blue.

It is observed from Table (1) that all salinity Indicators concentrate on using four spectral channels: R, G, and B, in addition to the near-infrared channel. This is due to the intensity of reflection of visible and near-infrared waves when they encounter salts (Elnaggar, 2009).

By applying these Indicators to the study area images, it was found that the most effective Indicator in identifying the most saline areas is the Salt Indicator 5, which is consistent with the results of a study (Rubab, 2016). It was followed in accuracy by the SI11 Indicator. The accuracy of the indicators was determined through visual comparison between the results of each Indicator and high-resolution visual imagery available in the ESRI Imagery Base Map. Figure (2) illustrates the results of applying the salinity Indicators to the saline plains in the Navigation Sabkha, the largest sabkha in the study area. It was found that while the salinity Indicators accurately identify the saline areas, they still only depict a portion of the sabkha surface, not the entire area. Therefore, it was necessary to search for a complementary Indicator to the salinity Indicator, and naturally, this Indicator was the water Indicator based on the nature of the phenomenon.

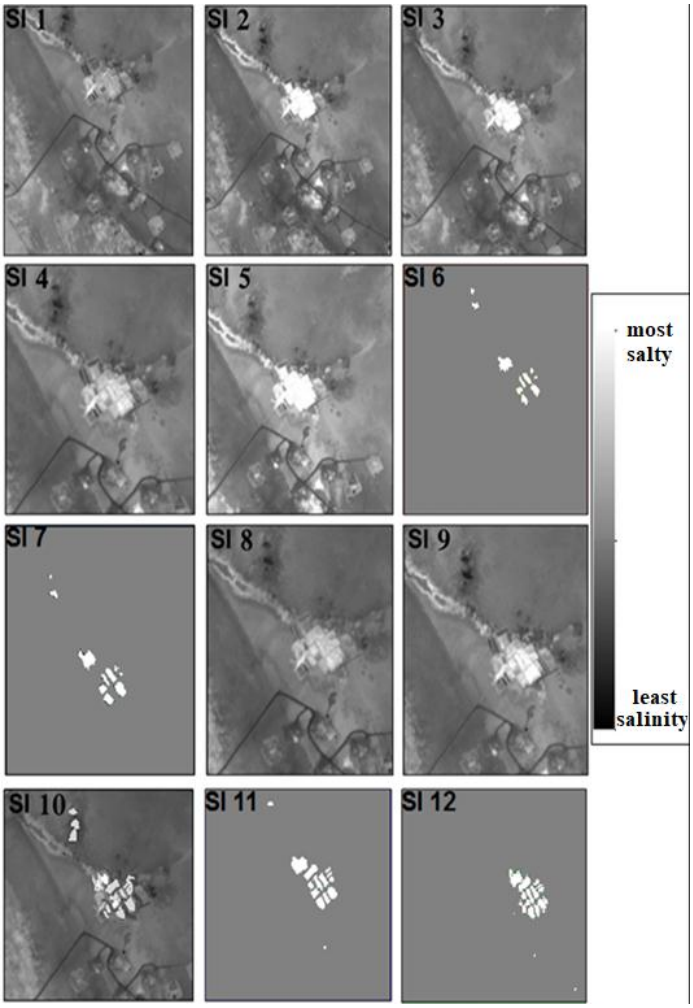

Figure (2): Results of applying different salinity Indicators.

2.2.3. Water Indicators:

Applying water Indicators in the study area faces two main challenges: the presence of shadows on the slopes and adjacent plains, as well as the similarity between some water bodies located on the coast, such as coastal lakes, and the surfaces of buildings surrounding them. The effectiveness of Indicators in overcoming these conditions varies, and the study sought to determine the most suitable Indicators to address these challenges. Based on the studies that have addressed water Indicators, several Indicators can be applied, including:

-NDWI (Normalized Difference Water Indicator)

-MNDWI (Modified Normalized Difference Water Indicator)

-IWS (Indicator of Water Surfaces)

-DFI (Desert Flood Indicator)

-AWEI (Automated Water Extraction Indicator)

2.2.3.1. Normalized Difference Water Indicator (NDWI)

Introduced by McFeeters (1996), the NDWI is the first water Indicator that uses the green and near-infrared (NIR) spectral bands to highlight water bodies effectively (bars, 2014). It is calculated using the equation: NDWI = (Green - NIR) / (Green + NIR). However, when applied to Landsat 5 TM imagery, the NDWI had a weak capability to differentiate between water surfaces, shadows, buildings, and roads.

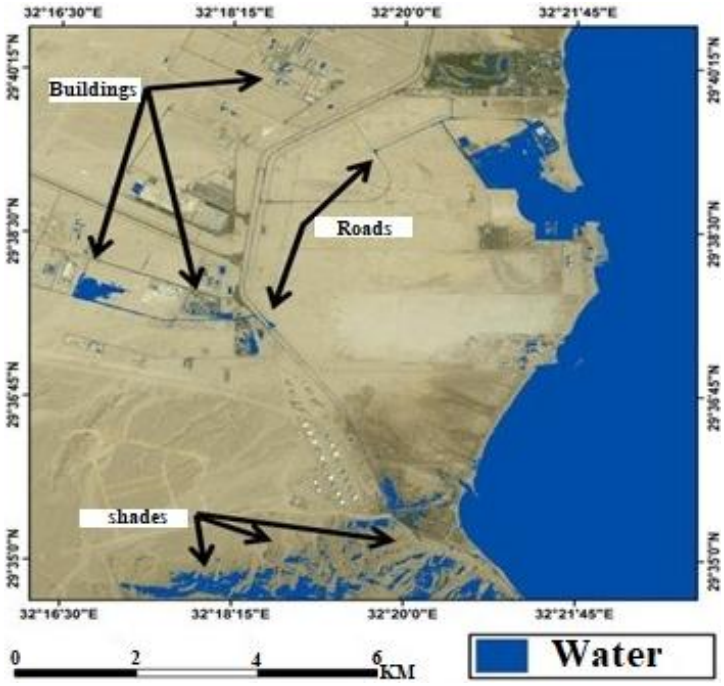

Figure (3): Results of applying the NDWI Indicator for water surface delineation.

2.2.3.2. Modified Normalized Difference Water Indicator (MNDWI)

Xu (2006) developed the MNDWI Indicator as a modification of the NDWI by replacing the NIR band with the mid-infrared (MIR) band. The equation is as follows: MNDWI = (Green - MIR) / (Green + MIR). This modification gives water higher positive values compared to the NDWI because water absorbs MIR wavelengths more than NIR wavelengths, while soil and vegetation have negative values because they reflect MIR wavelengths more than NIR wavelengths (Jensen, 2004). The MNDWI Indicator is widely used in remote sensing applications, including land use and land cover mapping. However, it has a significant limitation in distinguishing between water surfaces and built-up areas, as shown in Figure.(4)

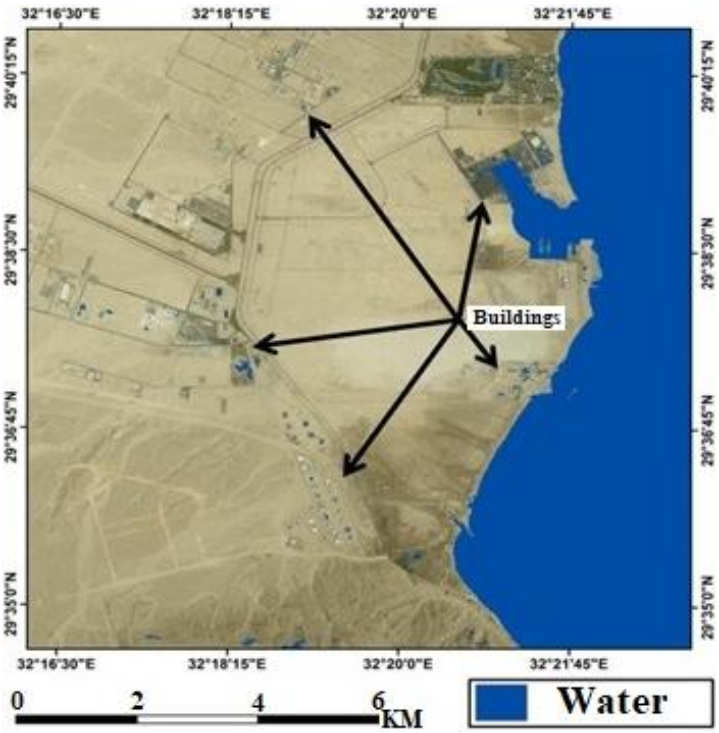

Figure (4): Results of applying the MNDWI Indicator for water surface delineation.

It can be observed that almost every building surface in the area contains blue points, which are misclassified as water bodies by the indicator.

2.2.3.3. Indicator of Water Surfaces (IWS)

The Indicator of Water Surfaces (IWS) was developed by Mohamed (2013) and applied to Landsat 7 imagery. It is calculated using the following equation:

IWS = (((4 * MIR - blue) * 2) / MIR) - ((2 * MIR) / blue). Liquid water strongly absorbs MIR wavelengths, while blue light is highly reflected (Mohamed, 2009). Applying this equation to the study area revealed that the indicator often fails to differentiate between water bodies and salt flats. Additionally, it neglects small water bodies and shallow water surfaces, which are not displayed in the results, as shown in Figure (5). This Indicator differs from others as it is applied without converting the digital numbers (DN) to radiance values (Mohamed, 2009).

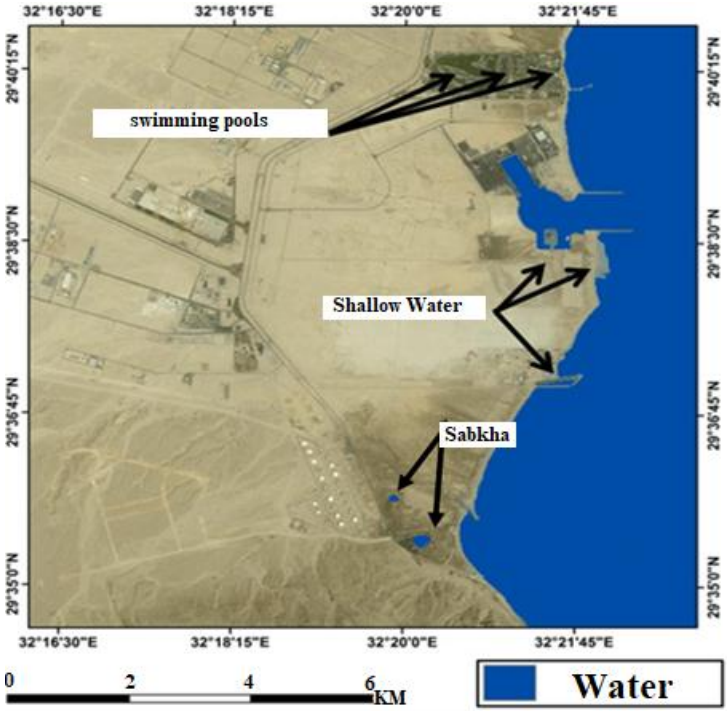

Figure (5): Results of applying the IWS Indicator for water surface delineation.

2.2.3.4. Desert Flood Indicator (DFI)

In the search for an Indicator that overcomes the limitations of the previous indices, Muhammad (2013) proposed the Desert Flood Indicator (DFI), which effectively distinguishes between agriculture, dark-colored soils, and water bodies. For example, it can differentiate between water-saturated lands and water bodies. The DFI is applied to Landsat 7 imagery using the following equation: DFI = (Green - SWIR + 0.1) / ((Green + SWIR) * (NDVI + 0.5)). The inclusion of NDVI in the equation helps to reduce the influence of vegetation reflectance, enabling better discrimination between water, marshes, and salt flats. Figure (6) shows the results of applying this equation.

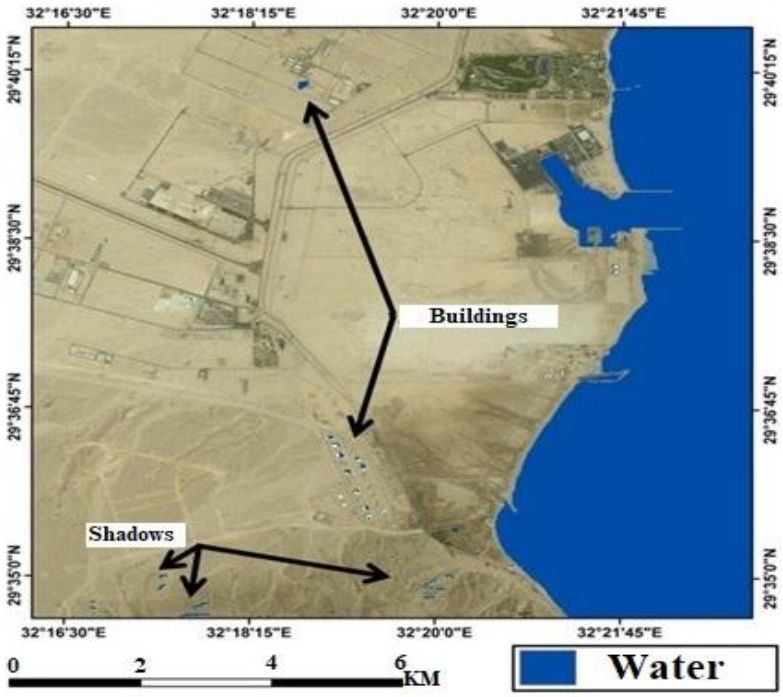

Figure (6): Results of applying the DFI Indicator for water surface delineation.

It can be observed that there is some overlap between shadows, elevated surfaces, buildings, and water bodies. Although this occurs to a lesser extent, it remains a limitation of the Indicator's results.

2.2.3.5. Automated Water Extraction Indicator (AWEI)

(Gudina, 2014) derived the AWEI Indicator, and the equation applied to this Indicator is as follows:

AWEInsh = 4*(Green - SWIR) - (0.25*NIR + 2.75*SWIR)

Figure (7) demonstrates that water bodies are distinct from adjacent dark building surfaces. The Indicator effectively separates shadows from water bodies and increases the contrast between them. This is confirmed through overlaying with the ESRI Imagery Base Map.

Thus, based on visual analysis of the results of these indices, it can be concluded that the AWEInshIndicator is the most effective in extracting water bodies. This is despite (Gilmore, 2015) claiming that the Modified Normalized Difference Water Indicator (MNDWI) is the best. However, this difference could be attributed to variations in the study areas. The current study area is a dry environment with less urbanization, unlike the wet urban complex of Dhaka, which was used in the study (Gilmore, 2015).

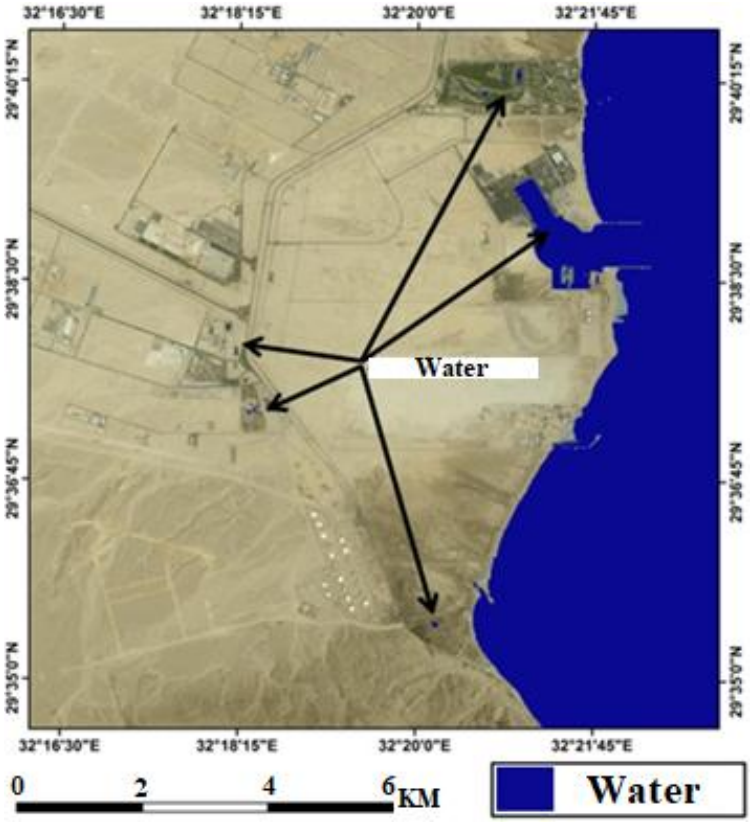

Figure (7) the results of applying the AWEInshIndicator to illustrate water bodies.

Different indices for water extraction were applied to the study area and compared visually. However, one step remains, which is quantitatively measuring the accuracy of each Indicator. This was done by delineating water bodies from high-resolution Google Earth imagery and performing an intersection between the delineation and the output of each Indicator separately. The percentage of water bodies not detected by the remote sensing Indicator compared to the water bodies delineated from high-resolution imagery was determined, resulting in Table.(2)

Table (2) the accuracy of each Indicator in extracting water bodies in the study area.

Indicator	The percentage of water bodies that the indicator didn't extract from the images to the existing water
NDWI	**%6.74**
MNDWI	**%4.11**
IWS	**%5.83**
DFI	**%5.07**
AWEI	**%3.91**

Based on the previous table, it can be concluded that the AWEI Indicator followed by MNDWI is the least in neglecting cells representing water in the remote sensing imagery, while the NDWI Indicator followed by IWS is the highest.

The actual number of cells representing water bodies was calculated among the cells generated by each Indicator and compared to the total number of cells resulting from the indicator in terms of a percentage. This produced Table (3), which represents the credibility of the results of different water indices.

Table (3) the credibility extent of the results of different water indices

Indicator	The percentage of cells that indicate water
NDWI	**%76.42**
MNDWI	**%87.64**
IWS	**%84.12**
DFI	**%81.55**
AWEI	**%89.88**

As a result of the above, it can be said that no single Indicator can suit all natural conditions in all regions. However, each Indicator has its advantages and disadvantages. If the correct Indicator is selected for the appropriate environment, the accuracy of the generated maps will certainly increase.

2.2.4. Sabkha Indicator:

Since the researcher found that the most suitable Indicator for application in the study area is the AWEInshIndicator, the salinity Indicator (SI5) was integrated with the water Indicator (AWEInsh) to create the Sabkha Indicator, which is calculated using the equation:

$$\text{SABKHA INDEX}=\sqrt{\text{AWEI}_{nsh}^{2}/\ \text{SI5}^{2}}$$

By applying this Indicator to the spectral channels of Sentinel-2 satellite imagery and using the thresholding technique, the sabkhas in the study area were extracted, as shown in Figure.(8)

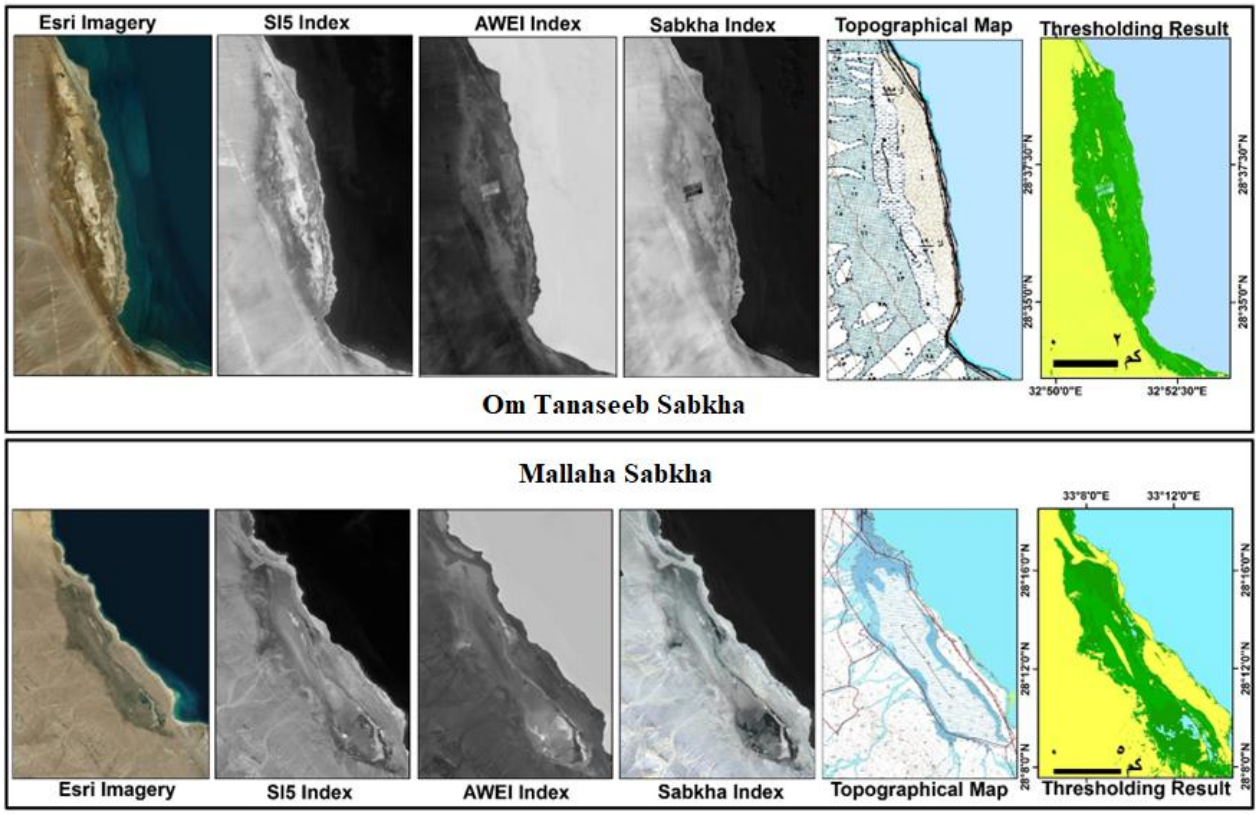

Figure (8) The extraction of sabkhas from Sentinel-2 satellite imagery.

3. Results and Discussions:

As a result of using the Sabkhas Indicator generated by the study, it has become possible to define the boundaries of the Sabkhas and monitor their growth and shrinkage throughout the year by tracking satellite images from various satellites and applying the indicator to them. By applying the Indicator to the Sabkhas located on the western coast of the Gulf of Suez, it was revealed that there are 24 different Sabkhas in terms of size and shape. These are the same Sabkhas found on topographic maps, with an accuracy reaching 78%. The 22% difference is attributed to the accuracy of the topographic maps and the difference in the survey date compared to the date of the satellite images used to apply the indicator. This is due to the inability to access the timing of field survey operations that resulted in the topographic maps. Additionally, the size of the Sabkhas can change over a year. To address this limitation, the study compared the results of applying the indicator with about 100 points surveyed through field studies. These evaluations were conducted using the Geotagged photos technique, which allowed the researcher to overlay the photographs taken during fieldwork on the results of

applying the indicator, resulting in an accuracy of 95% when comparing the results with the boundaries of the Sabkhas on the satellite images and topographic maps.

Analyzing the geographical distribution of the Sabkhas extracted from the satellite images revealed that the terrain conditions affect the Sabkhas, as the surface elevations and slopes vary. Regarding surface elevations, the decrease in the surface level in the coastal area allows seawater to penetrate these low-lying areas, forming the Sabkhas. As for the slopes, the Sabkhas spread and expand on the flat and gentle slopes that do not exceed 5 degrees, as shown in Table (4), which are available in the study area near the coast.

Table (4) the percentage distribution of Sabkha areas in different elevations and slope degrees.

Hight (M)	%	Slope (Degree)	%
-3 : 0	20	**0 : 2**	55
0 : 3	35	2 : 5	36
3 : 6	26	**5 : 10**	5
6 : 9	17	**10>**	4
13 : 9	2	_____	_____

The distribution reveals that there are 25 Sabkhas in the study area, with a total area of about 161 km2. The Navigation Sabkha occupies the largest area, with an area of 61 km2, while the Jiftun Al-KabeerSabkha occupies the last position with an area of not more than 0.06 km2. These Sabkhas are distributed along the Gulf of Suez in a semi-regular manner, although they tend to concentrate in the northern part. This can be explained by the higher surface elevation and the presence of elevated features such as Jebel Zeit and the Navigation Sabkha chain to the south. Table (5) illustrates the dimensions and characteristics of the Sabkhas in the study area.

Table (5) Dimensions of the Sabkhas in the study area.

Sabkha Name	**perimeter)KM(**	**Area)KM^2(**	**Elongation rate**	**Circularity rate**
wadiAlabar	17.6	2.81	0.49	0.11
Gabel Salmet	3.7	0.39	0.46	0.36
Om Tanaseeb	28.1	15.24	0.37	0.24
southern Garb Airport	13.5	2.76	0.39	0.19
Mallaha	63.1	61.03	0.40	0.19
North Wadi Dara	3.8	0.30	0.32	0.13
North Gareb Airport	2.4	0.21	0.41	0.16
MaghraHadira	4.1	0.23	0.71	0.17
Adabya	23.7	4.66	0.45	0.42

Ainsoukhna	24.3	5.67	0.36	0.12
Ghabat Al-Baws	26.2	9.36	0.76	0.17
Wadigraifat	16.2	4.38	0.40	0.21
Marsysalmet	28.9	11.13	0.32	0.17
Northern rasbakr	5.8	0.64	0.24	0.12
Rasbakr	21	8.19	0.37	0.23
Wadidara	8.7	0.78	0.32	0.13
Ghabat el-zait	45.6	20.14	0.43	0.14
Om Alkaiman	1.6	0.11	0.03	0.51
Northern Abo Gerfan	12.7	4.59	0.12	0.21
Jumusha	5.1	0.44	0.85	0.22
Abo Gerfan	24.3	7.47	0.50	0.21
Wadi al-esh	14.6	0.73	0.28	0.10
Jiftun Al-Kabeer	1.2	0.06	0.12	0.13
Om Haymat	4.7	0.16	0.40	0.09

From the previous table, the following points can be inferred:

-The Sabkhas vary in terms of area and perimeter, with the Navigation Sabkha recording the highest values in its dimensions.

-All Sabkhas extend in a general southeast to northwest direction towards the Gulf of Suez itself.

-Some Sabkhas terminate in coastal lakes because Gulf waters reached these locations during the Pleistocene epoch. Then, a gradual uplift occurred, resulting in the formation of a group of coastal lakes that occupied the axes of the Sabkhas. These lakes became isolated from the Gulf of Suez due to the continued uplift. During the Pleistocene epoch, these lakes received sediment from the wadis, which led to a reduction in their areas, especially during warm periods with high evaporation rates and the absence of a permanent water source to compensate for the loss. This resulted in a significant shrinkage in these lakes and the formation of the Sabkhas (Ahmed, 1984).

-Most of the Sabkhas tend to elongate, as they are Sabkhas that follow the coastline longitudinally. Except for Jumusha, Ghabat Al-Baws, and MaghraHadiraSabkhas, which are associated with the outlets of wadis.

-All Sabkhas are located away from the pivot except for Umm Al-Kayman Sabkha.

-Analysis of Landsat (T.M) satellite imagery in 1984 revealed that the southern Garb Airport Sabkha was part of the Navigation Sabkha. Parts of it were filled and cut off to build the Suez-Hurghada Road, turning Garb into a coastal Sabkha.

-Al-Adabiya Sabkha is a type of Sabkha that is associated with headlands. The shallow water of the Gulf of Suez, along with the extension of coral reefs, slows down the movement of water currents and leads to the formation of sandy ridges and lakes that transform into Sabkhas. On the other hand, Ghabat Al-BawsSabkha is a type of Sabkha associated with marine bays. It was

part of the bay and was filled with aeolian, alluvial, and clay deposits, with tributaries from Wadi Araba flowing into it (Iman, 2010).

-Umm TinasibSabkha has undergone morphological changes, with the disappearance of surface features associated with it due to human interventions in the area and the elevation of the Sabkha's surface.

-The field study indicated that the Navigation Sabkha is an exemplary Sabkha system, attributed to its morphometric dimensions that surpass any other Sabkha in the study area. Additionally, it exhibits morphological diversity in surface features associated with Sabkhas.

-Satellite images showed the disappearance and termination of some Sabkhas in the area due to human interventions, such as the eastern Jabal Abu Shaar Al-QibliSabkha, which vanished due to the construction of the El Gouna tourist resort (Figure 9).

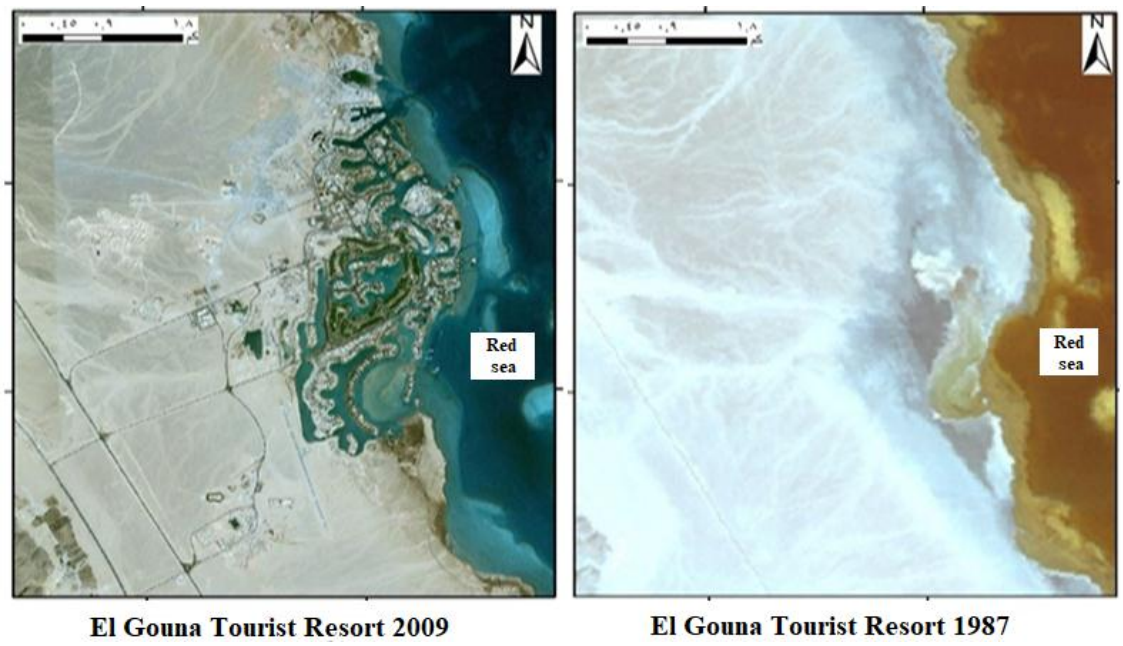

Figure 9: Impact of human intervention on the eastern Jabal Abu Shaar Al-QibliSabkha.

4. Conclusion:

The study utilized a set of Indicators applied to Sentinel-2 satellite imagery to determine the boundaries, areas, and morphometric characteristics of Sabkhas on the western coast of the Gulf of Suez. The study identified 24 Sabkhas with different characteristics. A specialized Indicator was developed to accurately extract the indicators from satellite images, achieving an accuracy of approximately 95%.

المستخلص

الخرائط الجيومورفولوجية الرقمية للسبخات غرب خليج السويس – مصر

محمد الراعي محمد

يلعب التخريط الرقمي للظاهرات الجيومورفولوجية دورًا مهمًا في تعيين حدودها. فلا تمتلك بعض الظاهرات حدودًا واضحة تفصلها عن محيطها، كما يمكن أن تتغير هذه الحدود مع ظروف المناخ المختلفة. لذلك؛ يفضل استخدام الأساليب الرقمية مثل، عمليات التصنيف بمختلف أنواعها وتطبيق المؤشرات لتعريف هذه الحدود. وتعد السبخات من أبرز الأمثلة على هذه الظاهرات؛ إذ يصعب تعيين حدودها ميدانيًا من ناحية، وتتغير حدودها باختلاف ظروف الطقس بشكل شبه يومي وبالتالي يصعب الاعتماد عل حدودها الموجودة على الخرائط الطبوغرافية من جهة أخرى. لذلك؛ يُفضل تحديد حدودها باستخدام صور الأقمار الصناعية التي يمكن أن تلتقط كل ثلاثة أيام أو أقل.

وعند سماع مصطلح "السبخة"، يتبادر إلى الذهن التربة التي تظهر فيها نسبة ملوحة عالية. وبالتالي يمكن استخلاصها من الصور الفضائية من خلال تطبيق مؤشرات الملوحة. إلا أنه وفي حالة المناطق الساحلية، تكون هذه السبخات مشبعة بالماء معظم الوقت. لذلك؛ كان من الضروري استخدام مؤشرات الملوحة والماء، أو مزيج منهما، لتعيين حدود هذه الظاهرة.

جدير بالذكر أن مؤشرات المياه تم استخدامها بدلاً من مؤشرات الرطوبة، وذلك لاعتماد مؤشرات الرطوبة على التغطية النباتية التي قد لا تكون متاحة طوال العام. بينما تتواجد المسطحات المائية طوال العام، وهكذا قدمت الدراسة مؤشرًا جديدًا مناسبًا لرسم خرائط السبخات بدقة.

وقد طبقت الدراسة هذه المؤشرات على مجموعة من السبخات الموجودة على الساحل الغربي لخليج السويس في مصر.

References

Abbas, A., Khan, S., 2007, Using Remote Sensing Techniques for Appraisal of Irrigated Soil Salinity. In L. Oxley, & D. Kulasiri (Eds.), Advances and Applications for Management and Decision-Making Land, Water, and Environmental Management: Integrated Systems for Sustainability MODSIM07, p. 2632-2638.

Ahmed, M, 1984, Geomorphological phenomena in the western coastal region of the Gulf of Suez, unpublished master's thesis, Faculty of Arts, Alexandria University

Barsi, J., Lee, K., Kvaran, G., Markham, B., Pedelty, J.,2014, The Spectral Response of the Landsat-8 Operational Land Imager. Remote Sens, p10232-10251. doi:10.3390/rs61010232.

Douaoui,A., Nicolas,H.,Walter,C.,2006, Detecting salinity hazards within a semiarid context using combining soil and remote-sensing data, Geoderma Volume 134, Issues 1–2, P 217-230.

Elnaggar, A., Noller, J., 2009, Application of remote-sensing data and decision-tree analysis to mapping salt-affected soils over large areas. Remote Sensing, 2(1), p 151-165.

Eman, A., 2010, Sabkhas in the Western bank of the Gulf of Suez by GIS, unpublished master's Thesis, Benha University, Egypt.

Gilmore, S., Saleem, A., Dewan, A., 2015, Effectiveness of DOS (DarkObject Subtraction) method and water Indicator techniques to map wetlands in a rapidly urbanizing megacity with Landsat 8 data, in Veenendaal, B., Kealy, A., (ed), Proceedings of Research@Locate in conjunction with the annual conference on spatial information in Australia and New Zealand, Vol-1323, Mar 10-12, 2015, pp. 100-108. Brisbane: CEUR-WS.

Goudie, A. (Eds.), Encyclopedia of Geomorphology. Routledge. London, p887-890.

Gudina, L., Henrik, M., Rasmus, F., Simon, R., 2014, Automated Water Extraction Indicator: A new technique for surface water mapping using Landsat imagery. Remote Sensing of Environment journal. DOI: 10.1016/j.rse.2013.08.029

JENSEN, J., 2004, Introductory digital image processing: A remote sensing perspective, 3rd edition (NJ: Prentice Hall Logicon Geodynamics, Inc).

Khan, M., Rastoskuev, V., Sato, Y., Shiozawa, S., 2005, Assessment of hydro saline land degradation by using a simple approach of remote sensing Indicators. Agricultural Water Management, 77(1–3), P96-109. doi: http://dx.doi.org/10.1016/j.agwat.2004.09.038

McFeeters, K., 1996, The use of Normalized Difference Water Indicator (NDWI) in the delineation of open water features. International Journal of Remote Sensing, 17, P.1425–1432.

Mohamed, M., Mohamed, H., Mohand, S., 2009, Indicator of extraction of water surfaces from Landsat 7 ETM+ images. Saudi Society for Geosciences, P. 3381–3389.

Muhammad, H., Lifu, Z., Shudong, W., Gaozhen, J., Shanlong, L., Qingxi, T., 2013, comparison of MNDWI and DFI for water mapping in flooding season. Institute of Remote Sensing Applications, Chinese Academy of Sciences, Beijing-100101, China

Rubab, A., Abdelgadir, A., 2016, COMPARATIVE ANALYSIS OF SALINITY INDICES FOR MAPPING SABKHA SURFACES IN THE UNITED ARAB EMIRATES, 37th Asian Conference on Remote Sensing, At Colombo, Sri Lanka.

Xavier, M., Paul, H., Silvia, C., Conor, C., 2015, Spatial Prediction of Coastal Bathymetry Based on Multispectral Satellite Imagery and Multibeam Data, International Journal of Remote Sensing, P.13782- 13806, doi:10.3390/rs71013782>

Xu, H. (2006). Modification of normalized difference water Indicator (NDWI) to enhance open water features in remotely sensed imagery. International Journal of Remote Sensing, 27